





Viacheslav LOVEIKIN ¹; Yuriy ROMASEVYCH ¹;
Andrii LOVEIKIN ²; Dmytro VELYKOIVANENKO ¹

Optimization of the joint start-up mode of the hoisting and slewing mechanisms of a boom

Received 18 January 2024, Revised 6 July 2024, Accepted 18 July 2024, Published online 4 September 2024

Keywords: tower crane, optimal control, metaheuristic, constraints, load pendulum oscillations

To increase the productivity of boom cranes, joint movement of mechanisms is performed. The simultaneous start-up of mechanisms significantly increases dynamic loads and intensifies oscillations of structural elements and loads on a flexible suspension reducing the reliability of crane operation and increasing energy losses. Therefore, the optimization problem of the joint start-up of the slewing and load hoisting mechanisms of a boom crane is stated and solved in the article. To optimize the joint start-up of the mechanisms, the boom system is represented by a 5-DOF dynamic model. For such a dynamic model of a boom crane, a mathematical model is developed in the form of a system of nonlinear differential equations of the second order. The optimization problem includes an optimization criterion and constraints on the driving torques and boundary conditions. An approximate modified metaheuristic PSO method was used to solve the nonlinear optimization problem. Based on the calculation, the optimal modes of joint start-up of the mechanisms for load slewing and hoisting of a boom crane were determined, making it possible to minimize dynamic loads and, as a result, reduce oscillations of the system links and energy consumption of the drives.

1. Introduction

To increase the productivity of boom cranes, the combined movement of several mechanisms is used. In particular, the joint movement of the slewing and load hoisting mechanisms is commonly applied. The case when both mechanisms simultaneously carry out transient processes (start-up, braking) is particularly dangerous for the boom crane operation. In such an instance, increased dynamic loads occur

✉ Yuriy ROMASEVYCH, e-mail: romasevichyuriy@ukr.net

¹National University of Life and Environmental Sciences of Ukraine, Kyiv, Ukraine

²Taras Shevchenko National University of Kyiv, Kyiv, Ukraine



in the crane's structural elements, and the energy consumption of the drive mechanisms increases. In addition, oscillatory processes happen in the crane structure elements, drive mechanisms, and the load on the flexible suspension. In this case, high-frequency oscillations in structural components and low-frequency spatial oscillations of the load on a flexible suspension are hazardous, affecting the crane's reliability and complicating the crane operator's work. Therefore, determining the optimal modes of joint start-up of the mechanisms for slewing and hoisting the load, which minimize dynamic loads and oscillatory processes in the elements of the crane boom system, is a promising area of research.

The operation of crane mechanisms and the crane system as a whole is significantly affected by transient processes (start-up, braking), during which additional dynamic loads occur in structural elements and drives [1–4], reducing the productivity and reliability of cranes and increasing energy losses. Considerable attention has been paid to the study of dynamic processes that occur during the operation of cranes. In [1, 2], modeling and dynamic analysis of tower cranes were performed, and in [3, 4], the dynamics of bridge cranes and container handlers were studied. These papers show a significant impact of dynamic loads on crane exploitation.

To increase the productivity of tower cranes, the movement of several individual mechanisms is combined. In paper [5] modelling and dynamic analysis of the joint movement of tower crane's slewing and trolley movement mechanisms were performed, which showed the overloading of the mechanisms and the presence of load oscillations on a flexible suspension. In [6], a mathematical model of the joint movement of the mechanisms for trolley movement, slewing, and hoisting was developed, based on which the dynamics of loads on the crane structural elements were estimated. The authors of [7] modeled and evaluated the impact of dynamic loads on the performance of a five-stage boom crane. The authors of [8] determined the effect of a load swinging on a flexible suspension on the dynamic loads impacting the drive mechanisms and structure of a double-boom crane. They controlled it with a PID controller with a nonlinear scheme. During the joint start-up of the mechanisms, oscillations of the load on the flexible suspension occur, which reduces the performance and reliability of tower cranes, so there is a need to study their dynamics during the simultaneous operation of crane slewing and load hoisting mechanisms. To reduce dynamic loads and prevent oscillations of crane structures and load on a flexible suspension, crane mechanisms are regulated during movement. Paper [9] analyzed the dynamical models of the tower crane. The stress is put on different pendulum effects (complex load oscillation) when ten 2D and 3D dynamical models are compared. The results of the work give the approach to reasonable selection of the tower crane dynamical model for the monitoring and control problems solution. The authors of [10] study a 4-DOF underactuated tower crane. To find the optimal control, a multiple time-step approach developed by the authors was applied. On each time step, a nonlinear model was linearized near the temporary operating point, then based on the algebraic Riccati equation solution H-infinity feedback controller was designed. The authors pointed out the

advantages of the approach. However, there was an obvious drawback – a huge volume of computation, which the control system should make on each time step. In the work [11], the characteristics and conditions of load oscillations and tower cranes construction vibrations in difficult conditions of crane work are considered. Paper [12] developed a non-model-based control of the tower crane, which was based on fuzzy logic. The obtained control provides optimal load positioning and reduces the load oscillations (but does not completely eliminate them). An important result of the study – is that only one state (position) can be considered. It, in turn, significantly reduces the complexity of the controller. The authors of [13] developed a mathematical model of a tower crane to eliminate load oscillations, which considers the boom's rotation and the hoisting of the load. The model is used to predict the oscillation frequencies during the simultaneous movement of mechanisms. In [14], the tower crane's load slewing mechanism is controlled by an artificial neural network. Here, the load oscillation is minimized by generating efficient input data. The methodology anticipates and adjusts the optimal control parameters based on the length of the flexible load suspension. The authors of the work [15], based on the observer, developed a control strategy, which suppresses the load oscillations in plane crane systems during hoisting and lowering of the load. In the article [16], a linear model of a bridge crane was used to solve the trajectory planning problem. Based on the S-shaped curve, a control law was found, which eliminates load's double pendulum oscillations. The author of the paper [17] solved the problem of global optimization of the ratio between the operation of the drive mechanisms of cranes. The author stated that findings may be used to reduce the dynamics forces on the crane structure. In [18], optimization criteria were obtained as quadratic functions for each tower crane mechanism, for which a minimization algorithm was developed, and optimal parameter values were determined to reduce the load on the crane structure and mechanisms. An approach similar to the previous one was designed in [19, 20], where optimization criteria in integral functionals are developed based on the differential equations of a single crane mechanism motion or the joint motion of several mechanisms. These functions represent the root mean square values of the driving torques, rate, and acceleration of their change in time [20] or a dimensionless reduction of these criteria in the form of a complex criterion [19]. By minimizing these functions, the optimal modes of crane mechanisms movement are determined, which reduce the load, oscillations, and energy consumption of cranes. Optimization of the operational modes of tower crane mechanisms leads to heightened productivity, enhanced reliability, and improved energy efficiency.

The analysis of studies concerning the joint operation of crane mechanisms shows a significant interest of researchers in the dynamic analysis of crane structures and their impact on crane efficiency. To achieve high crane efficiency, considerable attention is paid to solving dynamic optimization problems in operating individual mechanisms and their joint movement. The proposed work is devoted to the latter research area.

The system of joint movement of a boom crane's mechanisms is affected by the driving torques of the drive mechanisms, respectively, of slewing M_1 and hoisting M_2 , as well as the torque of resistance forces in the crane's slewing mechanism M_0 and the weight of the load with a gripping device and flexible suspension mg . Elastic forces act in the elastic elements of the drive mechanisms for slewing and hoisting. These are g – acceleration of free fall.

To develop a mathematical model of the dynamics of the joint movement of the hoisting and slewing mechanisms, represented by the dynamic model in Fig. 1, the Lagrange equations were used:

$$\begin{aligned}
 \frac{d}{dt} \frac{\partial T}{\partial \dot{\alpha}} - \frac{\partial T}{\partial \alpha} &= M_1 - \frac{\partial \Pi}{\partial \alpha}, \\
 \frac{d}{dt} \frac{\partial T}{\partial \dot{\beta}} - \frac{\partial T}{\partial \beta} &= M_2 - \frac{\partial \Pi}{\partial \beta}, \\
 \frac{d}{dt} \frac{\partial T}{\partial \dot{\varphi}} - \frac{\partial T}{\partial \varphi} &= -M_0 - \frac{\partial \Pi}{\partial \varphi}, \\
 \frac{d}{dt} \frac{\partial T}{\partial \dot{\psi}} - \frac{\partial T}{\partial \psi} &= -\frac{\partial \Pi}{\partial \psi}, \\
 \frac{d}{dt} \frac{\partial T}{\partial \dot{u}} - \frac{\partial T}{\partial u} &= -\frac{\partial \Pi}{\partial u},
 \end{aligned} \tag{1}$$

where T , Π are the kinetic and potential energies of the system, respectively; M_1 , M_2 are the driving torques of the slewing and hoisting drive mechanisms, reduced to the crane slewing column and the drive drum of the hoisting mechanism, respectively; M_0 – torque of resistance forces in the crane slewing part, reduced to the rotation axis.

The kinetic energy of the boom system during the joint movement of the slewing and hoisting mechanisms is represented as follows

$$T = \frac{1}{2} I_1 \dot{\alpha}^2 + \frac{1}{2} I_2 \dot{\beta}^2 + \frac{1}{2} I_3 \dot{\varphi}^2 + \frac{1}{2} m (\dot{u}^2 + \dot{\psi}^2 a^2), \tag{2}$$

where I_1 , I_2 are the moments of inertia of the drives of the crane and the drive drum of the hoisting mechanism reduced to the axes of rotation of the crane and the drive drum of the hoisting mechanism, respectively, of the slewing and load hoisting mechanisms; m is the mass of the load; I_3 is the moment of inertia of the crane's rotary part relative to its axis of rotation. In dependence (2), it is assumed that the deviation from the vertical of the flexible suspension has a negligible effect on the load's vertical hoisting rate.

Let us find the potential energy function of the system of joint movement of the slewing and load hoisting mechanisms,

$$\Pi = \frac{1}{2} C_1 (\alpha - \varphi)^2 + \frac{1}{2} C_2 [\beta r - n(u_0 - u)]^2 + mgy, \tag{3}$$

where C_1, C_2 – stiffness coefficients of the drive mechanisms for slewing and load hoisting are reduced in accordance with the axes of the crane rotation and the drive drum of the hoisting mechanism; r – radius of the drive drum of the hoisting mechanism; u_0 – length of flexible load suspension at the beginning of the movement; ν is the angular coordinate of the deviation from the vertical of the flexible load suspension.

Using the geometric relations from Fig. 1, we find the angular coordinate of the deviation from the vertical of the flexible load suspension ν :

$$\nu = a \frac{\varphi - \psi}{u}, \quad (4)$$

where a is the initial value of the load position.

We then determine the vertical coordinate of the center of mass of the load:

$$y = u_0 - u \cos \nu. \quad (5)$$

Let's find the partial and total derivatives of the kinetic energy (2) and the partial derivatives of the potential energy (3), which are included in Equation (1). In this case, in the expressions of partial derivatives of potential energy, we can assume that $\sin(\nu) = \nu$, since in actual operating conditions of boom cranes, the angular coordinate of deviation from the vertical of a flexible suspension with a load does not exceed 12° . Substituting the found expressions into system (1), we obtain a system of nonlinear differential equations for the joint movement of the boom crane's slewing and load hoisting mechanisms:

$$\begin{aligned} I_1 \ddot{\alpha} &= M_1 - C_1(\alpha - \varphi), \\ I_2 \ddot{\beta} &= M_2 - C_2 r(\beta r - n(u_0 - u)), \\ I_3 \ddot{\varphi} &= -M_0 + C_1(\alpha - \varphi) - m g a^2 \frac{\varphi - \psi}{u}, \\ m a^2 \ddot{\psi} &= m g a^2 \frac{\varphi - \psi}{u}, \\ m \ddot{u} &= -C_2 n(\beta r - n(u_0 - u)) + m g \left(1 + a^2 \frac{(\varphi - \psi)^2}{u^2} \right). \end{aligned} \quad (6)$$

When the load hoisting and slewing mechanisms are started together, significant dynamic loads occur in the crane structure, which intensifies oscillatory processes in its individual elements and the load on the flexible suspension. Dynamic loads largely depend on the magnitude and nature of the change in the driving torques of the drive mechanisms for load slewing and hoisting. Therefore, there is a need to determine the nature of the change in driving torques. This can be achieved by optimizing the mode of movement of the drive mechanisms for slewing the crane and hoisting the load, minimizing the effect of dynamic loads. As a criterion for optimizing the starting modes of the slewing and hoisting mechanisms, we use

the total dimensionless RMS value of the driving torques during the start-up time, which has the following form:

$$K_{ck} = \left\{ \frac{1}{t_1} \int_0^{t_1} \left[\delta \frac{M_1^2}{M_{1H}^2} + (1 - \delta) \frac{M_2^2}{M_{2H}^2} \right] dt \right\}^{1/2} \rightarrow \min. \quad (7)$$

Since with an increase in the value of the driving torques, the dynamic loads in the design of the crane boom system increase. Therefore, to reduce the dynamic loads in the crane hoisting and slewing mechanisms during their joint start-up, criterion (7) must be minimized. Criterion (7), which is an integral functional, must be minimized when the boundary conditions for the joint movement of the slewing and hoisting mechanisms are satisfied:

$$\begin{aligned} t = 0: \quad & \alpha = \frac{M_0}{C}, \quad \dot{\alpha} = 0, \quad \varphi = 0, \quad \dot{\varphi} = 0, \quad \psi = 0, \quad \dot{\psi} = 0, \\ & u = u_0, \quad \dot{u} = 0, \quad \beta = \frac{mg}{C_2nr}, \quad \dot{\beta} = 0, \\ t = t_1: \quad & \alpha = \frac{M_0}{C} + \frac{\omega t_1}{2}, \quad \dot{\alpha} = \omega, \quad \varphi = \frac{\omega t_1}{2}, \quad \dot{\varphi} = \omega, \\ & \psi = \frac{\omega t_1}{2}, \quad \dot{\psi} = \omega, \quad u = u_0 - \frac{vt_1}{2}, \quad \dot{u} = -v, \\ & \beta = \frac{mg}{C_2nr} + \frac{nvt_1}{2r}, \quad \dot{\beta} = \frac{n}{r}v \end{aligned} \quad (8)$$

along with the constraints on the driving torques of the crane slewing drives M_1 and hoisting drives M_2 :

$$M_{1 \min} \leq M_1 \leq M_{1 \max}, \quad (9)$$

$$M_{2 \min} \leq M_2 \leq M_{2 \max}, \quad (10)$$

where t is time; t_1 – the duration of the joint starting process of the slewing and hoisting mechanisms; ω is the steady-state angular velocity of the crane slewing column; v – steady-state linear speed of hoisting the load; δ – weight coefficient that takes into account the share of the driving torque of the slewing mechanism in criterion (7); M_{1H} , M_{2H} – rated values of the driving torques of the drives of the slewing and hoisting mechanisms, reduced to the axis of rotation of the crane and the axis of rotation of the drive drum of the hoisting mechanism, respectively; $M_{1 \max}$ and $M_{2 \max}$ – minimum and maximum allowable values of the driving torque of the slewing mechanism drive; $M_{2 \min}$ and $M_{2 \max}$ – the minimum and maximum permissible values of the driving torque of the hoisting mechanism drive.

In the optimization problem (7)÷(10), it is necessary to determine the modes of joint start-up of the boom crane's slewing and hoisting mechanisms, which minimize the complex dimensionless criterion (7) and provide boundary conditions (8) and limiting driving torques (9) and (10).

3. Problem solution

Let us express the integral criterion (7) through the generalized coordinates of the load rotation ψ and load hoisting u and their time derivatives. In order to do this, we express the driving torques of the drives, respectively, of the crane slewing and hoisting mechanisms from the first and second equations of system (6):

$$M_1 = I_1 \ddot{\alpha} + C(\alpha - \varphi), \quad (11)$$

$$M_2 = I_2 \ddot{\beta} + C_2 r (\beta r - n(u_0 - u)). \quad (12)$$

As a result of substituting the expression of the left-hand side of the fourth equation into the third equation of the system (6), we obtain

$$I_3 \ddot{\varphi} = -M_0 + C_1(\alpha - \varphi) - ma^2 \ddot{\psi}. \quad (13)$$

From equation (13), we express the angular coordinate of the drive of the slewing mechanism:

$$\alpha = \varphi + \frac{1}{C_1} (I_3 \ddot{\varphi} + ma^2 \ddot{\psi} + M_0). \quad (14)$$

Taking the time derivatives of expression (14) sequentially, we obtain the angular velocity and acceleration of the slewing mechanism drive:

$$\dot{\alpha} = \dot{\varphi} + \frac{1}{C_1} (I_3 \dot{\ddot{\varphi}} + ma^2 \dot{\ddot{\psi}}), \quad (15)$$

$$\ddot{\alpha} = \ddot{\varphi} + \frac{1}{C_1} (I_3 \overset{IV}{\ddot{\varphi}} + ma^2 \overset{IV}{\ddot{\psi}}). \quad (16)$$

Expressions (11)–(16) include the angular coordinate of the column of the slewing mechanism and its time derivatives, including the fourth order ones. Let us determine this coordinate from the fourth equation of system (6), as a result of which we have:

$$\varphi = \psi + \frac{u}{g} \ddot{\psi}. \quad (17)$$

Now let us take the time derivatives of expression (17) four times, and then we get:

$$\dot{\varphi} = \dot{\psi} + \frac{1}{g} (u \ddot{\psi} + \dot{u} \dot{\psi}), \quad (18)$$

$$\ddot{\varphi} = \ddot{\psi} + \frac{1}{g} (u \overset{IV}{\ddot{\psi}} + 2\dot{u} \dot{\ddot{\psi}} + \ddot{u} \dot{\psi}), \quad (19)$$

$$\overset{IV}{\ddot{\varphi}} = \overset{IV}{\ddot{\psi}} + \frac{1}{g} (u \overset{V}{\ddot{\psi}} + 3\dot{u} \overset{IV}{\ddot{\psi}} + 3\ddot{u} \dot{\ddot{\psi}} + \overset{IV}{\ddot{u}} \dot{\psi}), \quad (20)$$

$$\overset{IV}{\varphi} = \overset{IV}{\psi} + \frac{1}{g} \left(u \overset{VI}{\psi} + 4\overset{V}{\dot{u}} \overset{V}{\psi} + 6\overset{IV}{\ddot{u}} \overset{IV}{\psi} + 4\overset{IV}{\ddot{u}} \overset{IV}{\psi} + \overset{IV}{\dot{u}} \overset{IV}{\ddot{\psi}} \right); \quad (21)$$

After substituting expressions (14)÷(21) into dependence (11), we obtain the function of the driving torque of the slewing mechanism drive, which depends on the generalized coordinates of rotation ψ and hoisting u of the load and their time derivatives

$$M_1 = (I_1 + I_3 + ma^2)\overset{IV}{\ddot{\psi}} + \frac{(I_1 + I_3)}{g} \left(u \overset{IV}{\psi} + 2\overset{IV}{\dot{u}} \overset{IV}{\psi} + \overset{IV}{\dot{u}} \overset{IV}{\ddot{\psi}} \right) + \frac{I_1}{C_1} \left[(I_3 + ma^2) \overset{IV}{\psi} + \frac{I_3}{g} \left(u \overset{VI}{\psi} + 4\overset{V}{\dot{u}} \overset{V}{\psi} + 6\overset{IV}{\ddot{u}} \overset{IV}{\psi} + 4\overset{IV}{\ddot{u}} \overset{IV}{\psi} + \overset{IV}{\dot{u}} \overset{IV}{\ddot{\psi}} \right) \right] + M_0. \quad (22)$$

Using dependence (17) and making some transformations, the last equation of system (6) can be represented as follows:

$$C_2 r (\beta r - n(u_0 - u)) = m \frac{r}{n} \left(g - \ddot{u} + \frac{a^2}{g} \overset{IV}{\ddot{\psi}}^2 \right). \quad (23)$$

From equation (23), we determine the angular coordinate of the drive drum of the hoisting mechanism:

$$\beta = \frac{n}{r} (u_0 - u) + \frac{m}{C_2 n r} \left(g - \ddot{u} + \frac{a^2}{g} \overset{IV}{\ddot{\psi}}^2 \right). \quad (24)$$

Taking twice the time derivative of expression (24), we obtain the angular velocity and acceleration of the drive drum of the hoisting mechanism:

$$\dot{\beta} = -\frac{n}{r} \dot{u} + \frac{m}{C_2 n r} \left(-\ddot{u} + 2 \frac{a^2}{g} \overset{IV}{\ddot{\psi}} \overset{IV}{\dot{\psi}} \right), \quad (25)$$

$$\ddot{\beta} = -\frac{n}{r} \ddot{u} + \frac{m}{C_2 n r} \left[-\overset{IV}{\dot{u}} + 2 \frac{a^2}{g} \left(\overset{IV}{\ddot{\psi}}^2 + \overset{IV}{\dot{\psi}} \overset{IV}{\dot{\psi}} \right) \right]. \quad (26)$$

As a result of substituting expressions (23)÷(26) into dependence (12), we obtain the function of the driving torque of the hoisting mechanism, which depends on the coordinates of rotation ψ and hoisting u of the load and their time derivatives:

$$M_2 = I_2 \left\{ -\frac{n}{r} \ddot{u} + \frac{m}{C_2 n r} \left[-\overset{IV}{\dot{u}} + 2 \frac{a^2}{g} \left(\overset{IV}{\ddot{\psi}}^2 + \overset{IV}{\dot{\psi}} \overset{IV}{\dot{\psi}} \right) \right] \right\} + m \frac{r}{n} \left(g - \ddot{u} + \frac{a^2}{g} \overset{IV}{\ddot{\psi}}^2 \right). \quad (27)$$

To take into account the constraints (9) and (10) in the optimization problem (7)÷(10), we formulate a generalized criterion in the following form:

$$Cr = K_{CK} + I_{M_1 \min} + I_{M_1 \max} + I_{M_2 \min} + I_{M_2 \max} \rightarrow \min,$$

$$I_{M_1 \min} = \begin{cases} 0, & \text{if } \min(M_1) \geq M_{1 \min}, \\ \min(M_1) \delta_{M_1}, & \text{if } \min(M_1) < M_{1 \min}; \end{cases}$$

$$I_{M_1 \max} = \begin{cases} 0, & \text{if } \max(M_1) \geq M_{1 \max}, \\ \max(M_1) \delta_{M_1}, & \text{if } \max(M_1) < M_{1 \max}; \end{cases} \quad (28)$$

$$I_{M_2 \min} = \begin{cases} 0, & \text{if } \min(M_2) \geq M_{2 \min}, \\ \min(M_2) \delta_{M_2}, & \text{if } \min(M_2) < M_{2 \min}; \end{cases}$$

$$I_{M_2 \max} = \begin{cases} 0, & \text{if } \max(M_2) \geq M_{2 \max}, \\ \max(M_2) \delta_{M_2}, & \text{if } \max(M_2) < M_{2 \max}, \end{cases}$$

where $I_{M_1 \min}$ and $I_{M_1 \max}$ are the penalty components of the criterion responsible for satisfying the first and second inequality of constraints (9), respectively; $I_{M_2 \min}$ and $I_{M_2 \max}$ are the penalty components of the criterion accountable for satisfying the first and second inequality of constraints (10), respectively; δ_{M_1} and δ_{M_2} – weighting coefficients that determine the number of penalties for non-compliance with constraints (9) and (10), respectively (in the paper we use $\delta_{M_1} = 10^{10}$ and $\delta_{M_2} = 10^{10}$).

Let us reduce the boundary conditions (8) to the generalized coordinates of rotation ψ and hoisting u of the load and their time derivatives, resulting in

$$t = 0: \quad u = u_0, \quad \dot{u} = 0, \quad \ddot{u} = 0, \quad \ddot{\ddot{u}} = 0,$$

$$\psi = 0, \quad \dot{\psi} = 0, \quad \ddot{\psi} = 0, \quad \ddot{\ddot{\psi}} = 0, \quad \psi^{IV} = 0, \quad \psi^V = 0;$$

$$t = t_1: \quad u = u_0 - \frac{vt_1}{2}, \quad \dot{u} = -v, \quad \ddot{u} = 0, \quad \ddot{\ddot{u}} = 0,$$

$$\psi = \frac{\omega t_1}{2}, \quad \dot{\psi} = \omega, \quad \ddot{\psi} = 0, \quad \ddot{\ddot{\psi}} = 0, \quad \psi^{IV} = 0, \quad \psi^V = 0.$$
(29)

The complex dimensionless criterion (7), expressions (14)÷(27), and constraints (9) and (10) with boundary conditions (29) reflect an optimization problem. In this problem, it is necessary to determine the laws of change in the coordinates of rotation $\psi(t)$ and hoisting $u(t)$ of the load, which minimize criterion (7) and satisfy constraints (9), (10), and boundary conditions (29).

Since the above optimization problem is nonlinear, an approximate method is used to solve it, where the unknown functions $\psi(t)$ and $u(t)$ are represented by polynomials with two terms:

$$\psi(t) = \psi_1(t) + \psi_2(t), \quad (30)$$

$$u(t) = u_1(t) + u_2(t). \quad (31)$$

In expressions (30) and (31), the first terms $\psi_1(t)$ and $u_1(t)$ are selected polynomials that satisfy the boundary conditions (29), and the second $\psi_2(t)$ and $u_2(t)$ are the polynomials that include the free coefficients and satisfy the zero boundary conditions:

$$\begin{aligned} \psi_2(0) = \dot{\psi}_2(0) = \ddot{\psi}_2(0) = \overset{IV}{\psi}_2(0) = \overset{V}{\psi}_2(0) = 0, \\ \psi_2(t_1) = \dot{\psi}_2(t_1) = \ddot{\psi}_2(t_1) = \overset{IV}{\psi}_2(t_1) = \overset{V}{\psi}_2(t_1) = 0; \end{aligned} \quad (32)$$

$$\begin{aligned} u_2(0) = \dot{u}_2(0) = \ddot{u}_2(0) = \overset{IV}{u}_2(0) = 0, \\ u_2(t_1) = \dot{u}_2(t_1) = \ddot{u}_2(t_1) = \overset{IV}{u}_2(t_1) = 0. \end{aligned} \quad (33)$$

The function $\psi_1(t)$ is represented by an eleventh-order polynomial, and the function $u_1(t)$ – by the fifth order one. These functions satisfy the boundary conditions (28) and have the following form:

$$\psi_1(t) = \sum_{k=0}^{11} C_k t^k, \quad (34)$$

$$u_1(t) = \sum_{i=0}^7 D_i t^i. \quad (35)$$

Since in the boundary conditions (28), the time derivatives of the functions $\psi(t)$ and $u(t)$ are, respectively, of the fifth and third order, we will define them from functions (34) and (35), and then we obtain:

$$\begin{aligned} \dot{\psi}_1(t) &= C_1 + 2C_2t + 3C_3t^2 + 4C_4t^3 + 5C_5t^4 + 6C_6t^5 + 7C_7t^6 + 8C_8t^7 \\ &\quad + 9C_9t^8 + 10C_{10}t^9 + 11C_{11}t^{10}, \\ \ddot{\psi}_1(t) &= 2C_2 + 6C_3t + 12C_4t^2 + 20C_5t^3 + 30C_6t^4 + 42C_7t^5 + 56C_8t^6 \\ &\quad + 72C_9t^7 + 90C_{10}t^8 + 110C_{11}t^9, \\ \overset{IV}{\psi}_1(t) &= 6C_3 + 24C_4t + 60C_5t^2 + 120C_6t^3 + 210C_7t^4 + 336C_8t^5 \\ &\quad + 504C_9t^6 + 720C_{10}t^7 + 990C_{11}t^8, \end{aligned} \quad (36)$$

$$\begin{aligned} \overset{IV}{\psi}_1(t) &= 24C_4 + 120C_5t + 360C_6t^2 + 840C_7t^3 + 1680C_8t^4 + 3024C_9t^5 \\ &\quad + 5040C_{10}t^6 + 7920C_{11}t^7, \end{aligned}$$

$$\begin{aligned} \overset{V}{\psi}_1(t) &= 120C_5 + 720C_6t + 2520C_7t^2 + 6720C_8t^3 + 15120C_9t^4 \\ &\quad + 30240C_{10}t^5 + 55440C_{11}t^6; \end{aligned}$$

$$\begin{aligned} \dot{u}_1(t) &= D_1 + 2D_2t + 3D_3t^2 + 4D_4t^3 + 5D_5t^4 + 6D_6t^5 + 7D_7t^6, \\ \ddot{u}_1(t) &= 2D_2 + 6D_3t + 12D_4t^2 + 20D_5t^3 + 30D_6t^4 + 42D_7t^5, \\ \overset{IV}{u}_1(t) &= 6D_3 + 24D_4t + 60D_5t^2 + 120D_6t^3 + 210D_7t^4, \end{aligned} \quad (37)$$

where $C_0, C_1, \dots, C_{11}, D_0, D_1, \dots, D_7$ are the constants determined from the boundary conditions of the boom system movement (29).

After substituting the boundary conditions (29) with the coordinate ψ and its time derivatives into dependences (34) and (36), we obtain:

$$C_0 = C_1 = C_2 = C_3 = C_4 = C_5 = 0. \quad (38)$$

The constants C_6, C_7, \dots, C_{11} are determined from the system of linear equations:

$$\begin{aligned} C_6 + C_7 t_1 + C_8 t_1^2 + C_9 t_1^3 + C_{10} t_1^4 + C_{11} t_1^5 &= \frac{\omega}{2t_1^5}, \\ 6C_6 + 7C_7 t_1 + 8C_8 t_1^2 + 9C_9 t_1^3 + 10C_{10} t_1^4 + 11C_{11} t_1^5 &= \frac{\omega}{t_1^5}, \\ 30C_6 + 42C_7 t_1 + 56C_8 t_1^2 + 72C_9 t_1^3 + 90C_{10} t_1^4 + 110C_{11} t_1^5 &= 0, \\ 120C_6 + 210C_7 t_1 + 336C_8 t_1^2 + 504C_9 t_1^3 + 720C_{10} t_1^4 + 990C_{11} t_1^5 &= 0, \\ 360C_6 + 840C_7 t_1 + 1680C_8 t_1^2 + 3024C_9 t_1^3 + 5040C_{10} t_1^4 + 7920C_{11} t_1^5 &= 0, \\ 720C_6 + 2520C_7 t_1 + 6720C_8 t_1^2 + 15120C_9 t_1^3 + 30240C_{10} t_1^4 + 55440C_{11} t_1^5 &= 0. \end{aligned} \quad (39)$$

As a result of substituting the boundary conditions (29) with the coordinate u and its time derivatives in dependences (35), (37), we have:

$$D_0 = u_0, \quad D_1 = D_2 = D_3 = 0. \quad (40)$$

Other constants D_4, D_5, D_6, D_7 are determined from the following system of linear algebraic equations:

$$\begin{aligned} D_4 + D_5 t_1 + D_6 t_1^2 + D_7 t_1^3 &= \frac{v}{2t_1^3}, \\ 4D_4 + 5D_5 t_1 + 6D_6 t_1^2 + 7D_7 t_1^3 &= \frac{v}{t_1^3}, \\ D_4 + 10D_5 t_1 + 15D_6 t_1^2 + 21D_7 t_1^3 &= 0, \\ 4D_4 + 10D_5 t_1 + 20D_6 t_1^2 + 35D_7 t_1^3 &= 0. \end{aligned} \quad (41)$$

After substituting the constants (38) and (40), as well as those found as a result of solving the systems of linear algebraic equations (39) and (41) in the dependencies (34), (36), and (35), (37), we find functional dependencies that satisfy the boundary conditions (29) in the coordinates ψ and u and their time derivatives. Polynomials $\psi_2(t)$ and $u_2(t)$ will be represented in such a way as to satisfy the boundary conditions (32) and (33) and to equalize the free coefficients to the

same order:

$$\psi_2(t) = \left(\frac{t}{t_1}\right)^6 \left(\frac{t_1-t}{t_1}\right)^6 \sum_{k=0}^n A_k \left(\frac{t}{t_1}\right)^k \frac{\omega t_1}{2}, \quad 0 \leq t \leq t_1, \quad (42)$$

$$u_2(t) = \left(\frac{t}{t_1}\right)^4 \left(\frac{t_1-t}{t_1}\right)^4 \sum_{i=0}^p B_i \left(\frac{t}{t_1}\right)^i \frac{\nu t_1}{2}, \quad 0 \leq t \leq t_1, \quad (43)$$

where $A_0, A_1, \dots, A_n, B_0, B_1, \dots, B_p$ are free coefficients influencing the optimization criterion (28). Here, $\left(\frac{t}{t_1}\right)^6 \left(\frac{t_1-t}{t_1}\right)^6$ is a multiplier ensuring the satisfaction of zero boundary conditions (32) at arbitrary values of the coefficients A_0, A_1, \dots, A_n , for the coordinate ψ_2 ; $\left(\frac{t}{t_1}\right)^4 \left(\frac{t_1-t}{t_1}\right)^4$ is the factor that ensures the satisfaction of zero boundary conditions (33) at arbitrary values of the coefficients B_0, B_1, \dots, B_p for the coordinate $u_2(t)$. The coefficients $A_0, A_1, \dots, A_n, B_0, B_1, \dots, B_p$ are free and ensure that the minimum value of the criterion (28) is found.

As a result of substituting expressions (34)÷(43), taking into account the boundary conditions (29), in dependence (30) and (31), we obtain the expressions of functions $\psi(t)$ and $u(t)$ which include unknown free coefficients $A_0, A_1, \dots, A_n, B_0, B_1, \dots, B_p$.

Knowing the expressions of the functions $\psi(t)$ and $u(t)$ using dependencies (14), (17), and (24), we find the expressions of the angular coordinates of rotation of the drive mechanism $\alpha(t)$, the column $\varphi(t)$ and the drive drum of the hoisting mechanism $\beta(t)$ which also depend on the free coefficients $A_0, A_1, \dots, A_n, B_0, B_1, \dots, B_p$. When integrated, criterion (28) also becomes a function of the free coefficients $A_0, A_1, \dots, A_n, B_0, B_1, \dots, B_p$. Thus, the approximate solution of the optimization problem (7)÷(10), taking into account the replacement of boundary conditions (8) by conditions (29), is reduced to finding the minimum of the optimization criterion as a function of many variable free coefficients $A_0, A_1, \dots, A_n, B_0, B_1, \dots, B_p$.

To solve this optimization problem, we use the metaheuristic method VCT-PSO [21]. This algorithm has been successfully applied to solve a similar problem [22] and that is why we exploited it in the current study. The search domain for the coefficients is chosen from -200 to 200 . In this case, the generalized optimization criterion (28), taking into account expression (7), is represented by a function that depends on 12 free coefficients:

$$Cr = (A_0, A_1, \dots, A_5, B_0, B_1, \dots, B_3). \quad (44)$$

Calculations of optimal power modes of joint start-up of the boom crane's slewing and hoisting mechanisms according to the complex dimensionless criterion of the RMS value of driving torques (7) and constraints on the driving torques of

the drives of the mechanisms for slewing (9) and hoisting the load (10) while ensuring the boundary conditions for the movement of the mechanisms (29) are carried out at the following values of the parameters of the boom crane: $m = 2000$ kg; $I_1 = 71626.115$ kg·m²; $I_2 = 1249.93$ kg·m²; $I_3 = 4920738.85$ kg·m²; $M_0 = 39890$ Nm; $C_1 = 6.63 \cdot 10^6$ Nm/rad; $C_2 = 150796$ Nm/rad; $a = 30$ m; $v = 0.5$ m/s; $\omega = 0.075$ rad/s; $u_0 = 10$ m; $t_1 = 8.0$ s; $g = 9.81$ m/s²; $M_{1H} = 46625$ Nm; $M_{2H} = 3754$ Nm; $M_{1\min} = 0$; $M_{1\max} = 260000$ Nm; $M_{2\min} = 0$; $M_{2\max} = 14000$ Nm.

4. Research results

Upon solving the optimization problem, the following values of the free coefficients were obtained (Table 1).

Table 1. Optimization problem solutions

Coefficients	The value of the weighting factor δ		
	0.1	0.5	0.9
A_0	199.95	124.25	61.96
A_1	-167.88	-154.90	102.30
A_2	5.11	153.59	-200.00
A_3	179.18	-7.12	60.11
A_4	180.69	32.12	195.61
A_5	92.22	198.90	191.60
B_0	-35.17	-30.86	-27.56
B_1	42.65	46.66	82.07
B_2	34.42	-23.32	-121.46
B_3	-101.15	-29.47	52.83

To illustrate the minimization of criterion (44) for different variants of the weighting factor, we present plots (Fig. 2) that demonstrate the effective operation of the VCT-PSO algorithm [21]. Indeed, to overcome the penalty component (28) of criterion (44) and to ensure conditions (9) and (10), no more than fifty-six iterations are enough. Subsequently, the integral component of (7) is minimized. We find such values of criterion (7) when a further increase in the number of iterations (in our case, up to 200) does not lead to its change. These values of the criterion (7) are shown at different values of the coefficient δ in Fig. 2 by horizontal lines. Thus, we can conclude that the minimum values of criterion (7) have been found. This indicates that the optimization problem is solved.

As a result of solving the optimization problem of the combined process of starting the slewing and load hoisting mechanisms according to a complex dimensionless integral criterion, we obtained graphical dependences of the kinematic (Figs. 3–6), dynamic (Figs. 7, 8), and energy (Figs. 9, 10) characteristics of the

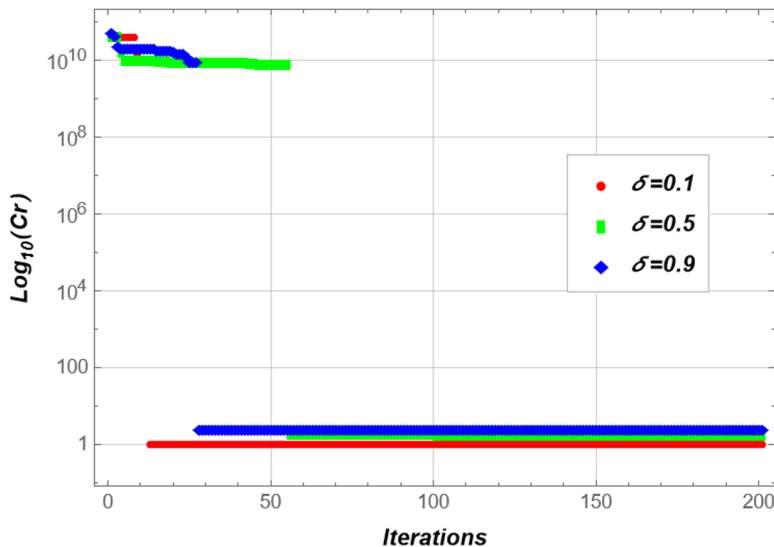


Fig. 2. Plot of minimization of criterion (44) when applying the VCT-PSO method, built in a logarithmic scale

tower crane boom system at three values of the weight coefficients and for basis solution (when all the coefficients $A_0, \dots, A_5, B_0, \dots, B_3$ equal to zero; it satisfies boundary conditions (8) and to some extent approximate of the optimization problem solution).

Fig. 3 shows that all dependencies of the slewing mechanism's angular velocity drive at three weight coefficient values change in the oscillatory mode. At the same time, larger values of oscillation amplitudes are observed at the beginning and end of the start-up process. The most significant oscillation amplitude of the angular velocity of the slewing mechanism drive is achieved at the end of the starting process at the weight coefficient $\delta = 0.1$. The best performance at the beginning of the start-up process is obtained by the mode at $\delta = 0.9$ at the end of the start-up mode – at $\delta = 0.5$. The angular speed of the hoisting mechanism drive (Fig. 4) changes smoothly in all four starting modes, but preference should be given to the starting mode at $\delta = 0.9$.

The phase trajectories of pendulum oscillations of a load on a flexible suspension (Fig. 5) show that during the start-up time, the load oscillations are eliminated in the motion modes corresponding to all three weight coefficients. The slightest deviation of the load rope from the vertical is achieved in the start-up mode when $\delta = 0.1$, but this launch mode also has the highest maximum deflection rate of the flexible suspension. In the other two optimal launch modes, the phase trajectories of the load's pendulum oscillations have almost the same change pattern. The worst features in this regard are observed at the basis solution, i.e., without optimization. The phase trajectories of elastic oscillations of the hoisting mechanism rope (Fig. 6) show that in all three optimal modes of movement, the oscillations are eliminated

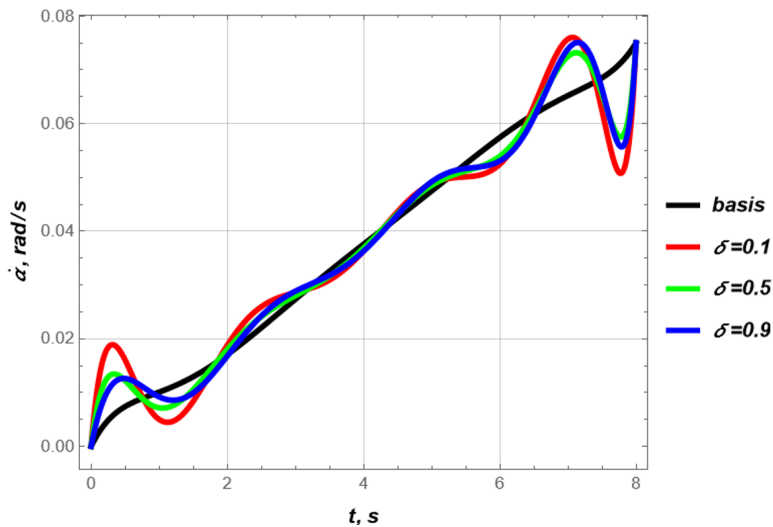


Fig. 3. Plots of the angular speed of the mechanism drive

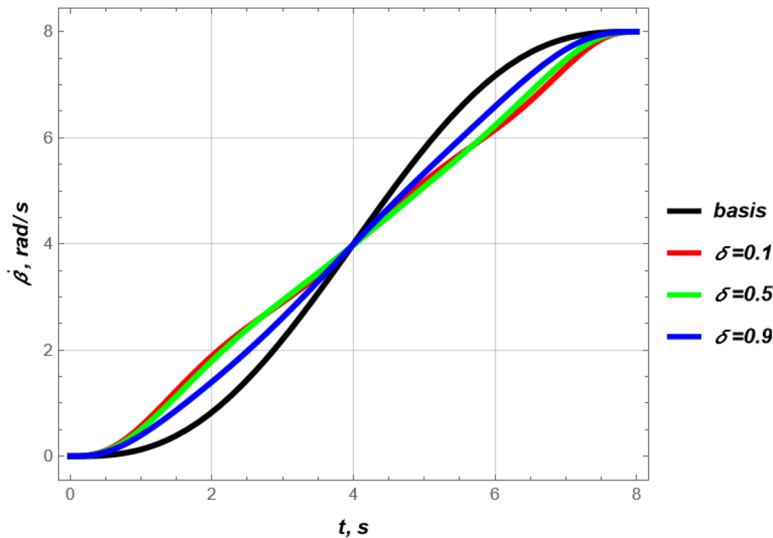


Fig. 4. Plots of the angular speed of the drive of the hoisting mechanism

during the start-up time. The phase trajectory has the smoothest change at the weight coefficient $\delta = 0.9$. The highest maximum rope deformation is obtained at the basis solution.

All the solutions provide pendulum oscillations of the load and elastic oscillations of the rope and crane column. However, Fig. 5 and 6 clearly show the superiority of optimization approach over unoptimized (basis) one.

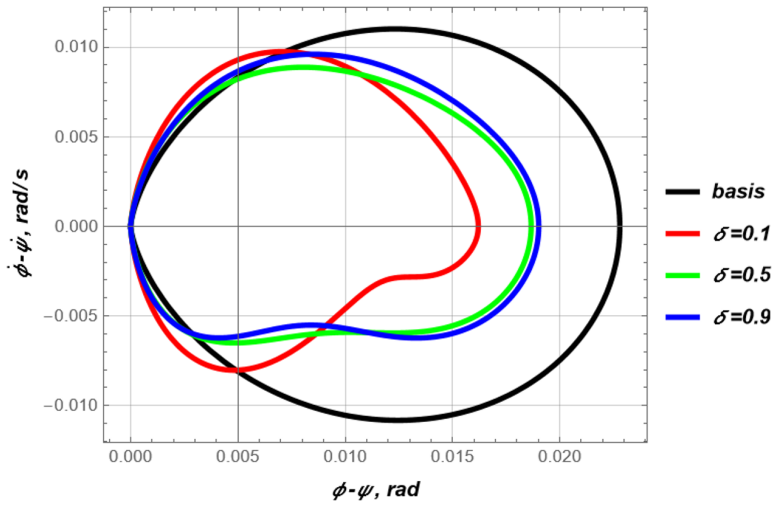


Fig. 5. Phase trajectories of pendulum oscillations of a load in a plane perpendicular to the crane boom

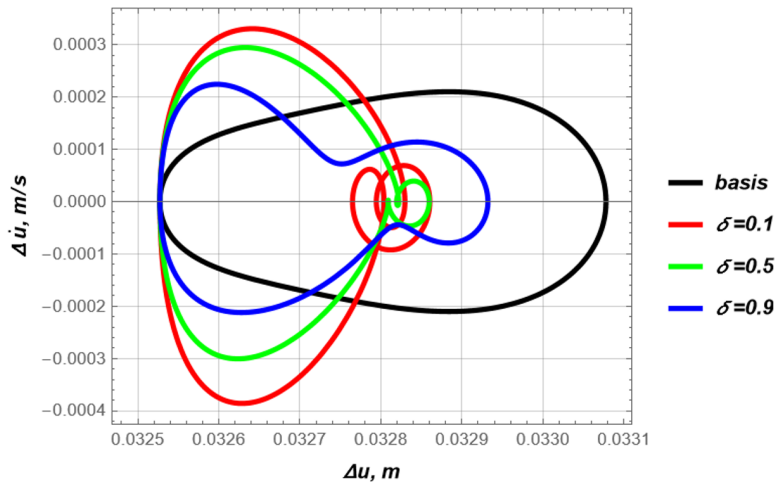


Fig. 6. Phase trajectories of elastic oscillations of the hoisting mechanism's rope

All four dependencies reach the same maximum value, corresponding to the drive torque maximum value (Fig. 7). In the middle part of the start-up process, the driving torque has a horizontal section, which is desirable for the driving torque. There are fluctuations in the driving torque at the beginning and the end of the start-up process for optimal controls. They allow us to minimize criterion (7) and satisfy constraints (9) and (10).

Fig. 8 and 9 show the smooth change in the driving torques for both of the mechanisms. For the case $\delta = 0.1$, the oscillatory manner of torques changes is observed. However, they do not lead to high-frequency oscillations in the elements

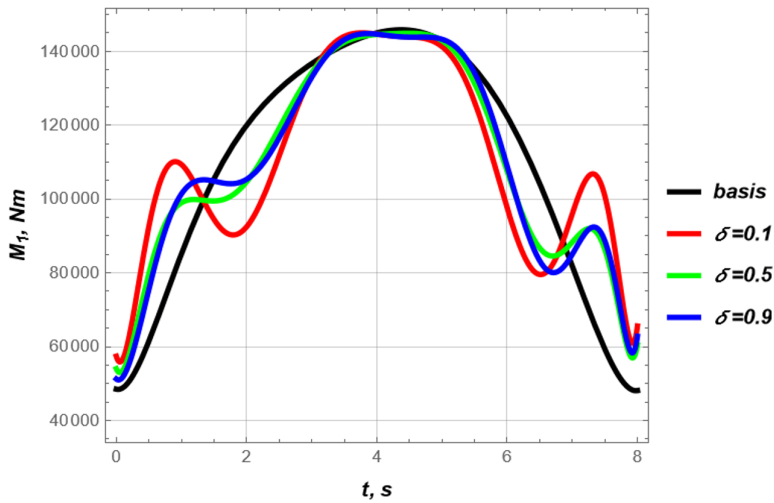


Fig. 7. Plots of the driving torque of the crane slewing mechanism

of the corresponding mechanisms (Fig. 5 and 6) after controlled mode end. For the hoisting mechanism, one may observe that the drive torque of the basis solution violates the constrain (10).

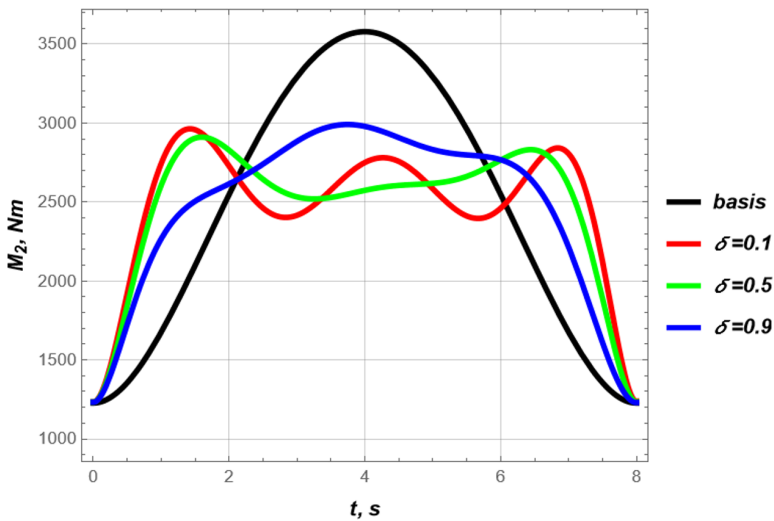


Fig. 8. Plots of the driving torque of the hoisting mechanism

The power of the slewing mechanism (Fig. 9) in all starting modes, which are determined by the weight coefficients, at the beginning and the end of the movement changes in an oscillatory mode, and in the middle part of the start, the power change is close to a linear law and practically does not depend on the value of the weight coefficient. The most significant amplitude of oscillations is in the

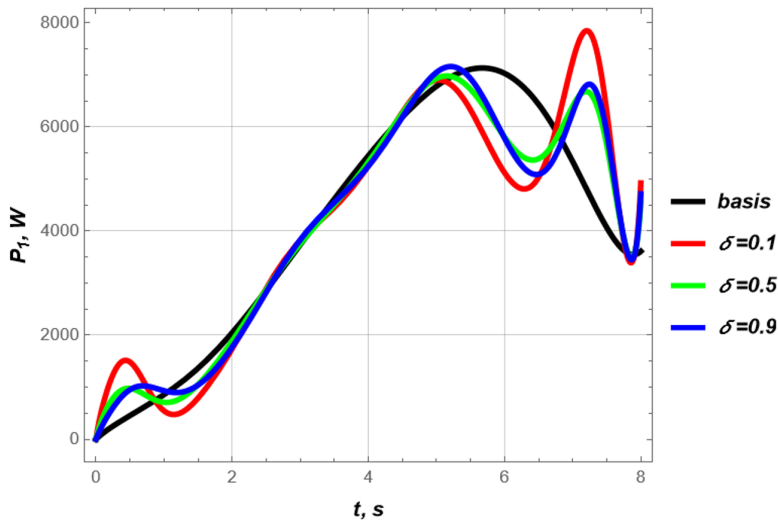


Fig. 9. Power plots of the crane slewing mechanism

starting mode at $\delta = 0.1$, and at $\delta = 0.5$, $\delta = 0.9$, and at the basis solution, the oscillation amplitudes are close to one another. The reason why at $\delta = 0.1$ power function such oscillates is connected with the oscillations of function $\dot{\alpha}$ (Fig. 3): its changes are the most significant compared to the cases $\delta = 0.5$ and $\delta = 0.9$.

Since the functions $\dot{\beta}$ (Fig. 4) and M_2 (Fig. 8) for all the cases of δ value do not differ significantly, the power functions (Fig. 10) are very close to each other. These functions smoothly change; their maximums are almost the same.

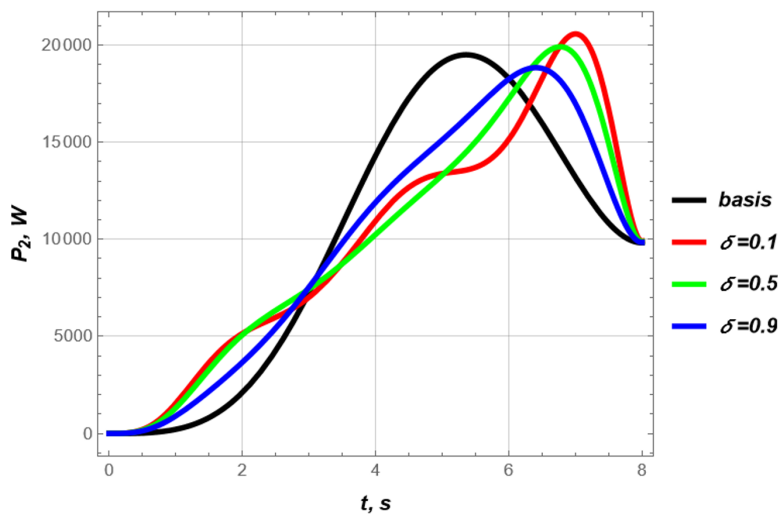


Fig. 10. Power plots of the hoisting mechanism

We also calculated numerical estimates of the obtained optimal movement modes of mechanisms at different values of the weighting coefficients in the complex dimensionless integral criterion (Table 2).

Table 2 shows the estimated indicators' RMS and maximum values for the three optimal starting modes corresponding to the weighting coefficients $\delta = 0.1$, $\delta = 0.5$, $\delta = 0.9$, and for the basis solution.

Table 2. Numerical estimates of the obtained optimal movement modes of mechanisms

Indicators	Unit of measurement	The value of the weighting factor δ			Basis solution
		0.1	0.5	0.9	
The extreme domain of indicators					
Power of the crane slewing mechanism	kW	7,844	6,975	7,157	7,130
Power of the load hoisting mechanism	kW	20,563	19,896	18,826	19,487
The total power of both mechanisms	kW	28,097	25,908	24,020	26,551
The driving torque of the crane slewing mechanism	kNm	144,980	144,885	144,774	145,820
The driving torque of the load-hoisting mechanism	kNm	2,963	2,910	2,991	3,578
Elastic deformation of the rope of the hoisting mechanism	m	0.0329	0.0329	0.0329	0.0331
Elastic deformation of a crane column	rad	0.0540	0.0590	0.0598	0.0219
Deviation from the vertical of a flexible load suspension	rad	0.0162	0.0187	0.0190	0.0228
RMS domain of indicators					
Power of the crane slewing mechanism	kW	4,699	4,682	4,687	4,722
Power of the load hoisting mechanism	kW	11,621	11,663	11,773	12,157
The total power of both mechanisms	kW	16,234	16,253	16,394	16,846
The driving torque of the crane slewing mechanism	kNm	113,066	113,413	113,526	114,961
The driving torque of the load-hoisting mechanism	kNm	2,510	2,513	2,530	2,612
Elastic deformation of the rope of the hoisting mechanism	m	0.0328	0.0328	0.0329	0.0331
Elastic deformation of a crane column	rad	0.0377	0.0387	0.0389	0.0172
Deviation from the vertical of a flexible load suspension	rad	0.0108	0.0113	0.0114	0.0124

According to the RMS power indicator, the lowest value is achieved for the slewing mechanism in the starting mode, which corresponds to $\delta = 0.5$ and the biggest one – at $\delta = 0.1$. The deviation between these indicators is 12.3%. For the hoisting mechanism, the lowest power is in the starting mode when $\delta = 0.9$, and the largest when $\delta = 0.1$, in the case of deviations between these indicators 9.2%. The total control of the two mechanisms has similar indicators: the lowest power corresponds to $\delta = 0.9$, and the highest one to $\delta = 0.1$. The deviation equals 17%.

The RMS value of the driving torque of the slewing mechanism drive for all four starting modes is almost the same. For the drive of the hoisting mechanism, the RMS value of the driving torque is the smallest when $\delta = 0.5$; the highest one corresponds to the basis solution. Thus, the provided optimization allows one to improve the dynamical features of the system in terms of decreasing of dynamical loads in the system elements.

The RMS value of the elastic deformation of the hoisting mechanism's rope for all four modes is almost the same. The only significant superiority of the basis solution is in the RMS of elastic deformation of a crane column. The worst load deflection in the plane perpendicular to the crane boom is for the basis solution, the best one – for the case $\delta = 0.1$ (Fig. 5), which is connected with fast changes of angular velocity (Fig. 3).

Let us evaluate the mechanisms' different starting modes by the maximum absolute value indicators. The smallest value of maximum power of the slewing mechanism corresponds to $\delta = 0.5$, and the highest one – to the basis solution. The difference in power indicators is insignificant, so all four modes may be considered equivalent in this regard. The same may be true for torque characteristics. Since the elastic deformation of the hoisting mechanism's rope is caused by the weight of the load, the maximum values for the four modes are almost the same.

The smallest maximum value of the elastic deformation of the crane column is at the basis control, and the highest one is at $\delta = 0.9$. However, for the load pendulum oscillations, the basis control is the worst one. The reason is the relatively slow increase of the angular velocity $\dot{\beta}$.

5. Conclusions

The study presents the results of optimizing the joint start-up of a tower crane's hoisting and slewing mechanisms with a hoisting boom. The joint operation of the tower crane mechanisms is represented by a dynamic model that considers the main movement of the drives of the hoisting and slewing mechanisms, elastic oscillations of the crane structure elements, and oscillations of the load on a flexible suspension. In total, the dynamic model is represented by a system with 5-DOF, for which the differential equations of motion are obtained. The coordinates of the links of the crane boom system are expressed through the linear coordinates of the horizontal and angular movement of the load. To minimize the dynamic loads on the structural elements of the crane boom system, an optimization problem was set in

which it was necessary to find the laws of motion of the crane hoisting and slewing mechanisms while minimizing the integral criterion and ensuring the required boundary conditions for the movement of the boom system links and constraints on the power characteristics of the drive mechanisms. Here, an integral functional is proposed as an optimization criterion, which is a dimensionless RMS value of the driving torques of the drives of the crane hoisting and slewing mechanisms, taking into account the weighting coefficients of each component of the criterion.

Since the optimization problem is nonlinear, an approximate method is used to solve it, which is represented by a generalized criterion taking into account the imposed constraints. When solving the optimization problem, the desired functions of the coordinates of the load horizontal movement and rotation are represented as polynomials with two terms. The first terms satisfy the boundary conditions for the joint mechanisms movement during the start-up process, and the second terms include free coefficients that satisfy zero boundary conditions. A modified metaheuristic PSO is applied to determine the free coefficients in the nonlinear optimization problem.

Based on the optimization, we have obtained the starting modes of hoisting and slewing mechanisms that minimize dynamic loads and eliminate oscillations of links and load when reaching the steady-state mode of mechanisms movement. From the above optimal starting modes at different values of the weighting coefficients in the complex integral criterion, it was found that the latter have different effects on individual estimated indicators, which vary from 0 to 18.8%. The most significant value of the deviation of the estimated indicator between the optimal starting modes is achieved for the total power of the drive mechanisms. The values of the weighting coefficients also significantly impact the smoothness of changes in the kinematic, dynamic, and energy characteristics of the crane boom system.

References

- [1] O. Grigorov, E. Druzhynin, V. Strizhak, M. Strizhak, and G. Anishchenko. Numerical simulation of the dynamics of the system "trolley-load-carrying rope" in a cable crane. *Eastern-European Journal of Enterprise Technologies*, 3(7(93)):6–12, 2018. doi: [10.15587/1729-4061.2018.132473](https://doi.org/10.15587/1729-4061.2018.132473).
- [2] V. Kovalenko, O. Kovalenko, V. Stryzhak, M. Stryzhak, and A. Ruzmetov. Determination of dynamic forces in the metal structure of tower crane based on the multi-mass model. *International Journal of Mechatronics and Applied Mechanics*, 14:248–256, 2023. doi: [10.17683/ijomam-issue14.29](https://doi.org/10.17683/ijomam-issue14.29).
- [3] N. Fidrovskaya, E. Slepuzhnikov, I. Varchenko, S. Harbuz, S. Shevchenko, M. Chyrkina, and V. Nesterenko. Determining stresses in the metallic structure of an overhead crane when using running wheels of the new design. *Eastern-European Journal of Enterprise Technologies*, 1(7(109)):22–31, 2021. doi: [10.15587/1729-4061.2021.225097](https://doi.org/10.15587/1729-4061.2021.225097).
- [4] M.M. Bello, Z. Mohamed, M.Ö. Efe, and H. Ishak. Modelling and dynamic characterization of a double-pendulum overhead crane carrying a distributed-mass payload. *Simulation Modelling Practice and Theory*, 134:102953, 2024. doi: [10.1016/j.simpat.2024.102953](https://doi.org/10.1016/j.simpat.2024.102953).

- [5] M. Zhang. Model-free finite-time trajectory tracking control for overhead cranes considering model uncertainties, parameter variations, and external disturbances. *Transactions of the Institute of Measurement and Control*, 41(12):3516–3525, 2019. doi: [10.1177/0142331219830157](https://doi.org/10.1177/0142331219830157).
- [6] O.S. Podolyak, O.M. Khoroshilov, and K.K. Anenko. Mathematical modeling of the joint movement of mechanisms for lifting, turning and changing the crane's departure. *Engineering*, 28:18–25, 2022 (in Ukrainian). doi: [10.32820/2079-1747-2021-28-18-25](https://doi.org/10.32820/2079-1747-2021-28-18-25).
- [7] M. Ambrosino, M. Berneman, G. Carbone, R. Crépin, A. Dawans, and E. Garone. Modeling and control of 5-DoF boom crane. *2020 Proceedings of the 37th International Symposium on Automation and Robotics in Construction*, pages 514–521, Kitakyushu, Japan, 2020. doi: [10.22260/ISARC2020/0071](https://doi.org/10.22260/ISARC2020/0071).
- [8] N. Sun, T. Yang, Y. Fang, Y. Wu, and H. Chen. Transportation control of double-pendulum cranes with a nonlinear quasi-PID scheme: design and experiments. *IEEE Transactions on Systems, Man, and Cybernetics: Systems*, 49(7):1408–1418, 2019. doi: [10.1109/TSMC.2018.2871627](https://doi.org/10.1109/TSMC.2018.2871627).
- [9] B. Johns, E. Abdi, and M. Arashpour. Dynamical modelling of boom tower crane rigging systems: model selection for construction. *Archives of Civil and Mechanical Engineering*, 23(3):162, 2023. doi: [10.1007/s43452-023-00702-x](https://doi.org/10.1007/s43452-023-00702-x).
- [10] G. Rigatos, M. Abbaszadeh, and J. Pomares. Nonlinear optimal control for the 4-DOF underactuated robotic tower crane. *Autonomous Intelligent Systems*, 2(1):21, 2022. doi: [10.1007/s43684-022-00040-4](https://doi.org/10.1007/s43684-022-00040-4).
- [11] F. Lui, J. Yang, J. Wang, and C. Liu. Swing characteristics and vibration feature of tower cranes under compound working condition. *Shock and Vibration*, 2021:8997396, 2021. doi: [10.1155/2021/8997396](https://doi.org/10.1155/2021/8997396).
- [12] A.B. Alhassan, W. Assawinchaichote, H. Zhang and Y. Shi. Hybrid input shaping and fuzzy logic-based position and oscillation control of tower crane system. *Expert Systems*. 41(2): e13484, 2024. doi: [10.1111/exsy.13484](https://doi.org/10.1111/exsy.13484).
- [13] J. Ye and J. Huang. Control of beam-pendulum dynamics in a tower crane with a slender jib transporting a distributed-mass load. *IEEE Transactions on Industrial Electronics*, 70(1):888–897, 2023. doi: [10.1109/TIE.2022.3148741](https://doi.org/10.1109/TIE.2022.3148741).
- [14] S.M. Fasih, Z. Mohamed, A.R. Hussain, L. Ramli, A.M. Abdullahi, and W. Anjum. Payload swing control of a tower crane using a neural network-based input shaper. *Measurement and Control*, 53(7-8):1171–1182, 2020. doi: [10.1177/0020294020920895](https://doi.org/10.1177/0020294020920895).
- [15] R. Miranda-Colorado. Robust observer-based anti-swing control of 2D-crane systems with load hoisting-lowering. *Nonlinear Dynamics*, 104:3581–3596, 2021. doi: [10.1007/s11071-021-06443-x](https://doi.org/10.1007/s11071-021-06443-x).
- [16] H. Ouyang, J. Hu, G. Zhang, L. Mei, and X. Deng. Decoupled linear model and s-shaped curve motion trajectory for load sway suppression control in overhead cranes with doublependulum effect. *Proceedings of the Institution of Mechanical Engineers, Part C: Journal of Mechanical Engineering Science*, 233(10):3678–3689, 2019. doi: [10.1177/0954406218819029](https://doi.org/10.1177/0954406218819029).
- [17] S. Chwastek. Finding the globally optimal correlation of cranes drive mechanisms. *Mechanics Based Design of Structures and Machines*, 51(6):3230–3241, 2023. doi: [10.1080/15397734.2021.1920978](https://doi.org/10.1080/15397734.2021.1920978).
- [18] S. Chwastek. Optimization of crane mechanisms to reduce vibration. *Automation in Construction*. 119:103335, 2020. doi: [10.1016/j.autcon.2020.103335](https://doi.org/10.1016/j.autcon.2020.103335).
- [19] V. Loveikin, Y. Romasevych, I. Kadykalo, and A. Liashko. Optimization of the swinging mode of the boom crane upon a complex integral criterion. *Journal of Theoretical and Applied Mechanics. Sofia*, 49:285–296, 2019. doi: [10.7546/JTAM.49.19.03.07](https://doi.org/10.7546/JTAM.49.19.03.07).
- [20] V. Loveikin, Y. Romasevich, A. Loveikin, and A. Khoroshun. Optimizing the start of the trolley mechanism during steady slewing of tower crane. *International Applied Mechanics*, 58(5):594–604, 2022. doi: [10.1007/s10778-023-01183-4](https://doi.org/10.1007/s10778-023-01183-4).

- [21] Y. Romasevych, V. Loveikin, and Y. Loveikin. Development of a PSO modification with varying cognitive term. *2022 IEEE 3rd KhPI Week on Advanced Technology (KhPIWeek)*, pages 1–5, Kharkiv, Ukraine, 2022. doi: [10.1109/KhPIWeek57572.2022.9916413](https://doi.org/10.1109/KhPIWeek57572.2022.9916413).
- [22] V. Loveikin, Y. Romasevych, A. Loveikin, M. Korobko, and A. Liashko. Minimization of oscillations of the tower crane slewing mechanism in the steady-state mode of trolley movement. *Archive of Mechanical Engineering*, 70(3):367–385, 2023. doi: [10.24425/ame.2023.146847](https://doi.org/10.24425/ame.2023.146847).